Ultrasonic Agitation for Emerging Electrodeposition Systems

S. Roy and S.J. Coleman

Department of Chemical and Process Engineering, University of Strathclyde, James Weir Building, Glasgow G1 1XJ. Contact: Sudipta.roy@strath.ac.uk

Introduction

Despite the growing importance of electrodeposition for the development of new materials for energy applications [1], sensor fabrication [2], micro and nano-fabrication [3, 4], the technologies used in these processes remain reliant mostly on traditional methods as rack and barrel plating. In the first half of the twentieth century, agitation in these systems were achieved by cathode movement or air sparging [5]. The systematic introduction of eductors [5], the paddle cell and fountain flow for wafer plating [6], and a jet plating system to selectively plate metal at a particular location [7] were major innovations of the final quarter of the past century.

Whilst these changes and other academic studies [5-12] testify the importance of agitation during an electrodeposition process, there have been fewer explorations of agitation in the current century. Notwithstanding, over the past two decades there have been new developments in electrodeposition, such as electrochemical printing [13, 14] and mask-less microfabrication [15, 16], which required unconventional agitation schemes as a core need for the process to work. The electrochemical printing method used new jetting technology to deliver fluids, which required precise control over jet placement, fluid viscosity and surface tension [13, 14]. Electrochemical mask-less microfabrication, required that the anode and cathode to be placed within 500 μm [17] whilst maintaining good agitation. These developments required new thought for agitating fluids during electrodeposition and understanding them sufficiently to enable the design of new systems. Ionic liquids [18, 19], which have been proposed as the next generation of electrolytes for metal deposition, which are highly viscous [18, 19] and corrosive [20], will also require new approaches for agitation. If conventional methods

were used to pump the electrolyte, pump ratings would need to increase by at least one order of magnitude, and pump material would need to be corrosion proof.

Ultrasonic (*US*) agitation can provide a way forward for agitation of electrochemical systems [21, 22]. For example, it is possible that viscous fluids could be displaced using *US*, thereby eliminating mechanical pumps and contact with corrosive liquids. *US* agitation using miniature probes could be used to pulsate fluids and through small channels enabling jet flow. For the case where the space between electrodes is constrained, there is the possibility of focusing the flow within the gap. Figure 1 illustrates the last idea: (a) traditional pumping *vs.* (b) US probe focusing flow within the gap.

In this paper we describe the deployment of *US* to increase agitation in constrained spaces. In particular, here we describe the adaptation and changes needed for measurement of mass transfer rates. The use of *US* using horns (or probes) as well as tanks for electrodeposition has been described. Specifically the two systems correspond to laboratory scale measurement and industrial scale apparatus. By constrained space we have limited ourselves to a narrow gap between two electrodes [23], mostly in the mm scale.

Ultrasonic Agitation for Electrodeposition

Ultrasonics has already been used in electrodeposition of metals to improve deposits, current efficiency and improve material distribution [24-26]. Enhancement of mass transfer has been detected while studying the effect of *US* streaming on oxide films [27] while others have decoupled mass transfer enhancements caused by US [22, 28, 29]. There have also been attempts to analyse agitation using probes in a face-on [29] and side-on systems [30], and mass transfer boundary layer thickness based on these measurements have been quantified [29, 30].

(a)

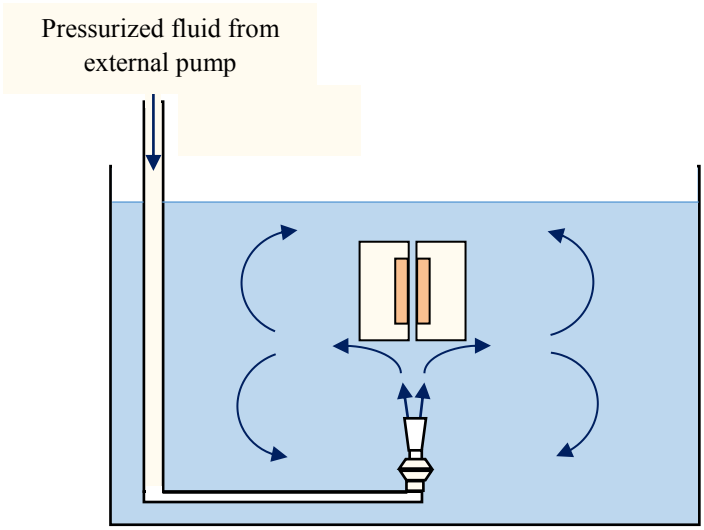

(b)

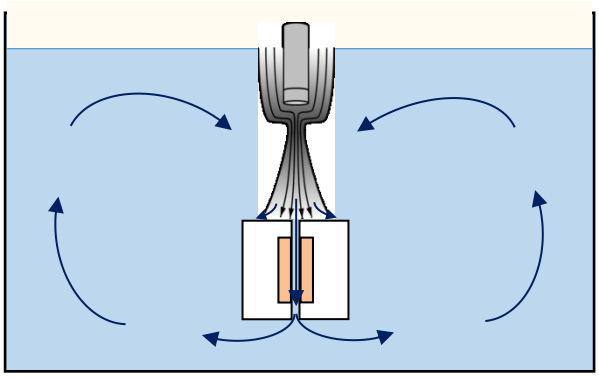

Figure 1: Schematic of electrolyte flow around narrow electrode gap using (a) eductor agitation, (b) ultrasonic agitation. In (a) the high velocities by-pass the interior of the gap, whereas pressure waves could travel through the gap in (b).

Here we explain the approach taken by the authors to address an important question: Can US be employed to increase material transport within constrained spaces, i.e. a narrow gap [16, 23]? At this point, it is unclear to what extent agitation could be improved; furthermore, it was not even evident if experimental techniques such as the limiting current method, could be applied in these

circumstances. In fact, other researchers had already found that there are distortions in potential distribution due to the presence of an US probe [31].

Mass transfer Measurement in a Laboratory Scale System

Since the effect of material transport within a narrow gap using *US* was not known, the starting point for our analysis was to examine if an experimental system, which could accommodate closely placed anode, cathode, reference electrode and *US* horn could be designed. Figure 2 shows a laboratory scale system used by our group, where two electrodes were placed in close proximity within a cylindrical reservoir. The distance between the two electrodes could be controlled via a screw system, and the system was calibrated so that we could adjust the gap reasonably accurately. The *US* probe was placed above it to focus the *US* agitation directly within the gap. The *US* system (*SONICS Vibra-Cell VC505 Processor*) with a Titanium alloy tip was operated at a fixed frequency of 20 kHz, and the power was varied between 9-29 W/cm^2 (25-75 W L^{-1}).

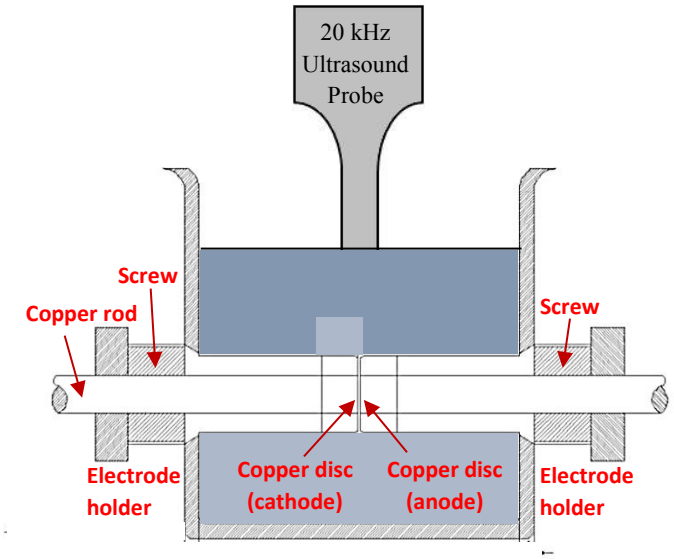

Figure 2: Experimental set-up of the electrochemical cell used with ultrasound probe placed directly above a narrow electrode gap. (Adapted from [32])

The detail for the placement of the reference is shown in Figure 3. A reference probe could not be placed within the inter-electrode gap, because this could cause a disturbance in the electric field between the two electrodes. Therefore, a reference probe was placed 5 mm above and to the side of the gap. The design of the electrochemical cell allowed one to assess the effect of two different parameters: (1) the inter-electrode gap which defined the constrained space, and (2) probe-to-electrode distance which controlled the power delivered into that space. The placement of the reference above the plane of the anode and cathode, as well the insertion of the US tip (or horn), which can serve as a third electrode, are departures from a standard three-electrode set-up used for limiting current measurement.

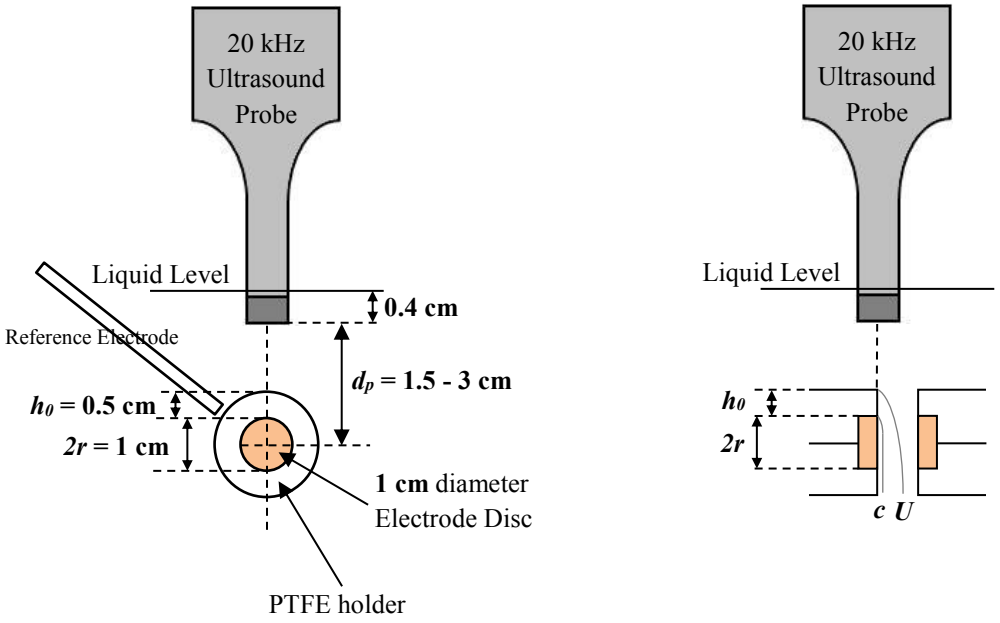

Figure 3: Dimensions of the probe and the placement of a reference electrode. The placement of the probe and the development of the momentum and concentration boundary layers along the length of the electrode is indicated. Here *c* is concentration and *U* is flow velocity. Adapted from [32].

The methodology in the limiting current technique employs the collection of current vs potential data. When an electrochemical reaction is kinetically controlled, current increases with applied potential. As mass transfer limitations are encountered, the current remains nearly constant with increasing potential, and is called the limiting current plateau. The mass transfer boundary layer, δ, is related to the plateau current, called the limiting current, by the following equation

$$|i_L| = n\,F\,D\,\left({}^{C_b}/_{\delta}\right) \quad (1)$$

Here, i_L is the value of the limiting current, n is the number of electrons transferred, F is Faraday constant, D is the diffusion coefficient, and C_b is the concentration of reacting species in solution.

Figure 4 shows the limiting current data obtained for a 0.1 M $CuSO_4$/0.1 M H_2SO_4 electrolyte using this apparatus. The conditions for electrode gap, horn-to-electrode distance, d_p, and measurement conditions are provided in the caption. The oscillations in current are due to cavitation activity near the electrode surface. As the horn was brought closer to the inter-electrode gap, the current potential data show distortions, some of which show up as apparent hydrogen evolution commencing at a low overpotential. This distortion is caused by a third metallic, grounded electrode (horn) placed within the electrochemical cell [32]. However, limiting current plateaux were still identifiable, and they were used to determine the mass transfer boundary layer.

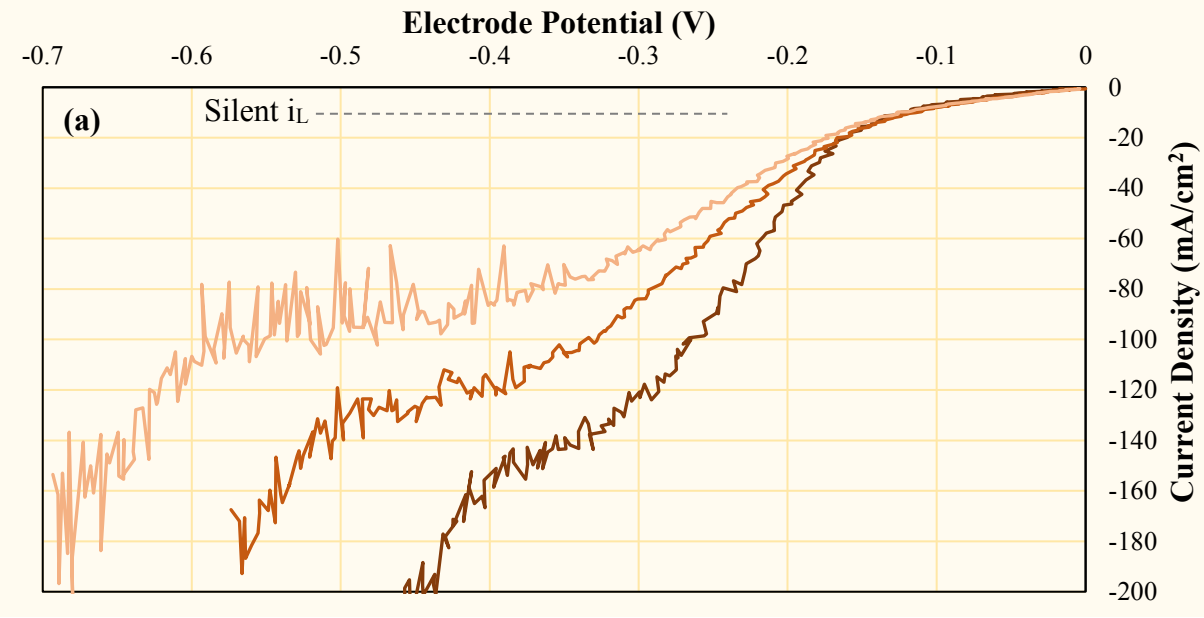

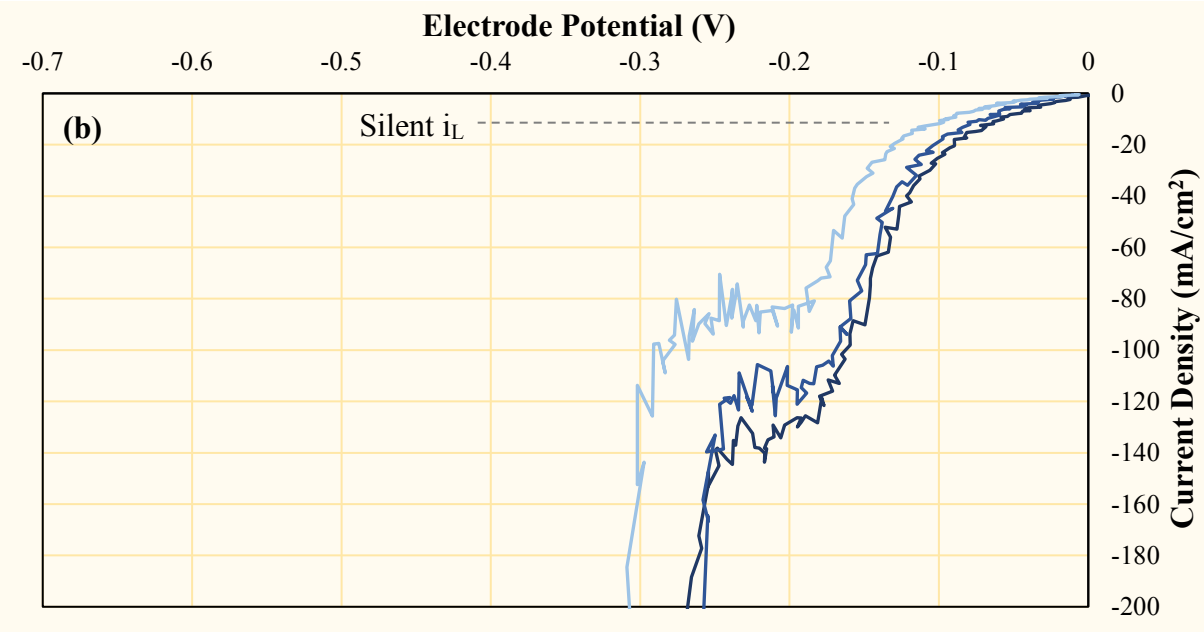

Figure 4 - Linear Potential scans with a 0.1 M $CuSO_4$ + 0. 1 M H_2SO_4 electrolyte; Scan Rate = 5 mV/s. (a) h_e = 0.5 cm ; at varying d_p of 3 cm (dashed light orange), 2 cm (orange) and 1.5 cm (red) at fixed p of 18 W/cm^2. (b) h_e = 0.15 cm, with same ultrasound conditions as for 'a' and varying d_p at distances of 3 cm (light blue), 2 cm (blue) and 1.5 cm (dark blue). Dotted line denotes the i_L under silent conditions, he = 0.5 cm. (Adapted from [32])

The limiting current data were used to develop mass transfer correlations within the constrained volume. Sherwood-Schmidt-Reynolds number correlations for different electrode gaps and horn-to-gap distances are listed below [32, 33]:

$$Sh = k_1 (Re.Sc.\frac{d_e}{L})^{0.82} \quad (2a)$$

$$Sh = k_2 (Re.Sc.\frac{d_e}{L})^{1.38} \quad (2b)$$

In these equations *Sh*, *Re* and *Sc* correspond to Sherwood, Schmidt and Reynolds numbers respectively, and d_e and L are the equivalent diameter and length, respectively. Equations 2a and 2b correspond to electrode gaps of 10 mm and 1.5 mm, respectively. These correlations show that for a wider gap, developing turbulence controls mass transfer. For the narrower gap, one obtains a fully turbulent condition, presumably due to eddies generated within the gap.

Mass Transfer Measurement in a Large Scale 18 Litre Tank System

Measurement of limiting current within industrial scale tank system is more complicated. There are two major issues – tank systems have lower power, and the power is very evenly distributed [34]. In addition, much of the earlier work has focused on high power to influence reaction chemistry, and studies related to microfabrication have shown that lower power may be more useful for electrodeposition [23, 24].

Figure 5 shows the design for the electrodes with a narrow gap within a tank system. The electrodes are placed at the centre of the tank, and connectors to the electrodes as well as the inter-electrode gap is maintained via the design of an appropriate holder which is described in detail elsewhere [33, 35]. The gap between the electrodes was set at 1.5 mm, achieved by placement of spacers in the corners and one in the centre of the plate. The tank was 18 L, and the electrode size

was 74 mm x 105 mm (A7 size), much larger than the lab scale system (which was of 10 mm diameter). The tank operated at 30 kHz and limiting current experiments were performed at 30, 40 and 60 WL^{-1}.

Figure 5 also shows the detail of anode and cathode used in these experiments. The cathode was a Perspex plate with a copper contact at the back. Two square slots 10 mm x 10 mm, near the centre and edge were made where copper inserts were placed, depending on the position where the limiting current had to be measured. The anode was an A7 size copper plate, the same size as the perspex plate. Limiting currents were measured via galvanostatic means. Although limiting currents would normally be measured potentiostatically, when such large electrodes are used, there can be significant potential distribution, which makes data difficult to interpret. Therefore, measuring an average current and cell potential to locate a plateaux current provides a practical method to determine limiting current in a tank-type reactor.

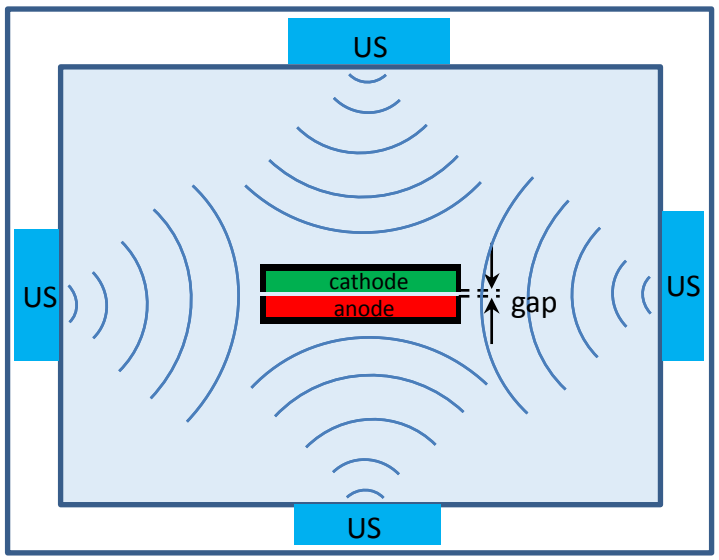

Top View

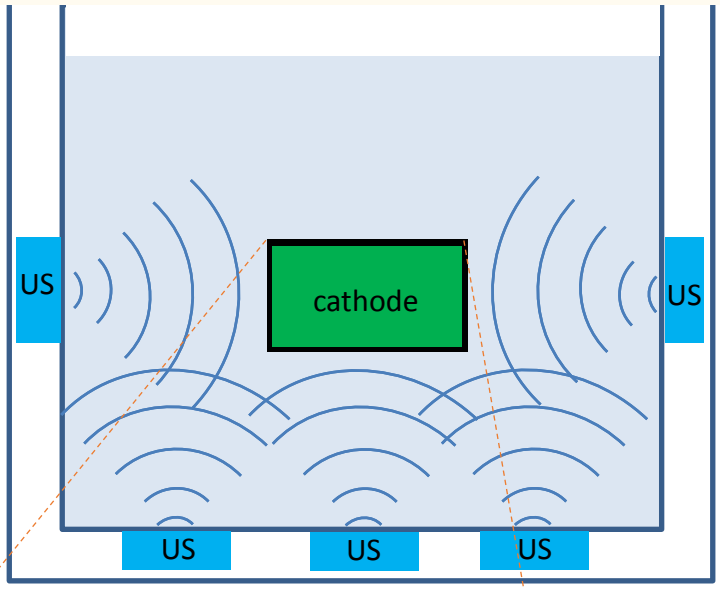

Side View

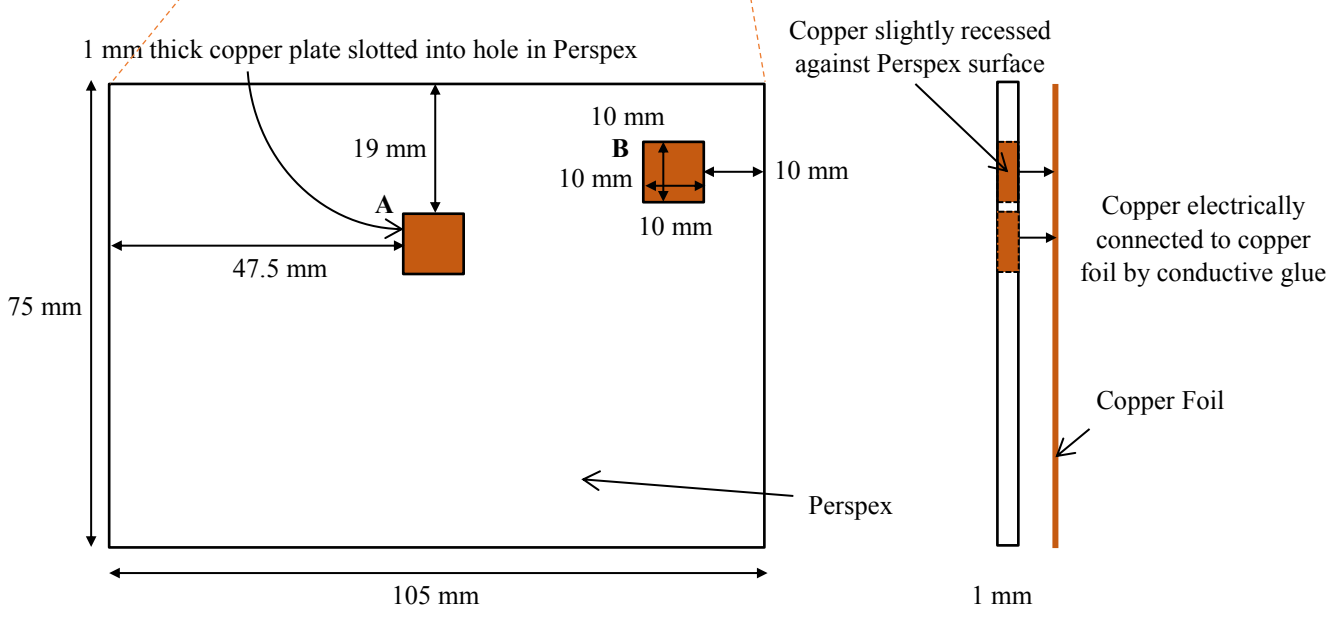

Figure 5: Electrode arrangement used for limiting current experiments in the *US* tank. Ultrasound transducers, indicated by *US*, show the arrangement in the 18 L tank. The limiting current was measured at location (A) and (B), i.e. at the centre and edge of the plate to detect differences in agitation.

The limiting currents at location (A) and (B), were determined to be similar; at location A, δ was found to vary between 15 μm and 19 μm, and it was 17 μm at location B, indicating that the variation in mass transfer at the edges and centre are not significant. The Sherwood-Schmidt-Reynolds number for this system was found to be [35]

$$Sh = \ k_3 (Re.Sc.\frac{d_e}{L})^{0.41} \quad (3)$$

These analyses show that whilst *US* tanks are capable of significantly increasing agitation within the narrow gap between electrodes of A7 size, the effect of *US* streaming is less pronounced. This tank system was used to carry out electrodeposition of copper structures at the micron scale, which required photolithographed substrates. It was found that powers higher than 10 WL^{-1} caused de-adhesion of the photomasks from substrates [23, 35]. It was found that low powers were favourable for microfabrication due to increased longevity of masks. Therefore, increasing mass transfer is not the sole criterion for optimisation of microfabrication systems.

Imaging

Whilst mass transfer correlations are useful chemical engineering tools for design, a closer inspection of mechanistic processes during US application is also necessary. Imaging techniques have previously been used to visualise cavitation and the phenomenon of micro-jetting using special photography [36]. The experiments managed to capture the precise moment of a cavitation bubble collapse and the formation of a micro-jet. There is also work using fluorescence microscopy to detect

microbubbles which have propagated from an ultrasound probe [37], studying the effect of collapsing bubbles on the surface of a cell.

Although it is crucial to quantify cavitation activity as a function of the process parameters, there are a limited amount of studies. A very interesting work on laser phase-Doppler technique was used to study bubble velocity, size distributions and volumetric flow of ultrasonic cavitation bubbles propagating from a 20 kHz ultrasound probe [38] in a 1.7 L tank and a free-flowing geometry. The experiments demonstrated that the jet from the probe had similar hydrodynamic properties to turbulent circular jet flows. The work also showed that ultrasound power increases bubble velocity quasi-linearly, and changes bubble diameter which were dependent on distances from the probe tip.

The current authors considered the feasibility of using optical techniques to visually capture the movement of cavitation bubbles within a narrow gap of <1 mm. An imaging technique was deemed feasible for a thin gap since light could be transmitted through the electrolyte in the gap, and be interpreted from transmitted images. Therefore a glass cell was constructed with borosilicate windows positioned (almost exactly) parallel to each other with a gap of <1 mm. A 20 kHz ultrasound probe was used as the ultrasonic source, and was placed 3 cm above the gap. The glass cell was filled with 500 ml of electrolyte, and the probe tip was dipped into the solution to generate *US* agitation. Although the full details of the imaging experiment is beyond the scope of this paper, other additional components required were a light source, a diffuser, slit, iris, 2 achromatic lenses, 2 mirrors, a razor blade and a Nikon D50100 camera.

Both Schlieren and Shadow Graph imaging were tested with the assistance of Prof. Patrick Bunton (visiting Professor from Vanderbilt University), of which, Shadow Graph appeared to provide reasonable images. One frame from the videos during the first few seconds of applying ultrasound at 23 W L^{-1} is shown in Figure 6. Although the camera used in this experiment operated at only 25 frames a second, the tracks of the streaming bubbles are discernible, shown by the dark vertical lines indicated by the arrows. It is known that ultrasonic cavitation effects can be captured using a

synchronized high-speed stroboscopic Schlieren imaging technique [39], using a cavitational trigger, such as sono-luminesence and cavitation noise. If a similar technique were used, it is likely that bubble movement within narrow gaps can be observed.

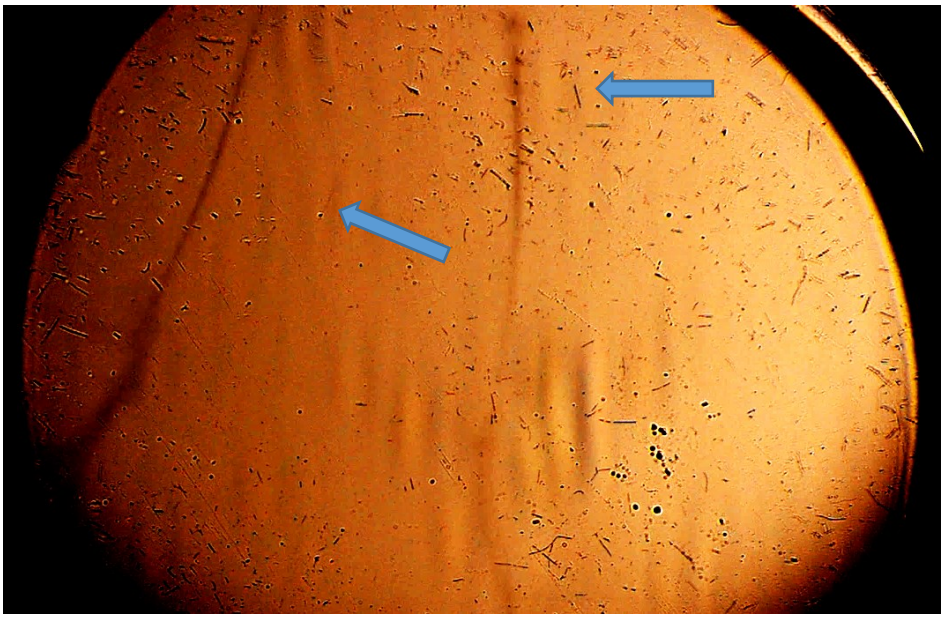

Figure 6 – Frame from video of shadow graph experiment showing traces of bubbles within a narrow gap of 1 mm with 23 W L^{-1} ultrasound power

Acknowledgements: The authors acknowledge the help of Prof. Patrick Bunton, University of Vanderbilt, for imaging experiments.

References

1. Osaka, T. and Datta, M. (2014). Energy storage systems in electronics. CRC Press.

2. Datta, M., Osaka T., Schulze J.W. (2005). Microelectronic Packaging. CRC Press: Boca Raton.

3. Madou, M.J. (2002). Fundamentals of microfabrication: the science of miniaturization. (eds.) CRC press: Boca Raton.

4. Datta, M., Landolt, D. (2000). *Electrochimica acta*, 45(15-16), pp. 2535-2558.

5. Gabe D.R. (2006). *Trans. Inst. Metal Finishing*, 84(2), pp. 67-78.

6. Ritzdorf T.L., Wilson G.J., Mchugh P.R., Woodruff D.J., Hanson K.M., Fulton D. (2005). *IBM J. Res: Dev*, 49(1), pp. 65-77.

7. Chin D.T. (2017). *J. Electrochem. Soc*., 138(9), pp. 2643 – 2650.

8. Selman, J.R., Tobias C. W. (1978). *Advances in Chemical Engineering*, 10(1) 1-318.

9. Wragg A.A., Ross T.K. (1967). *Electrochimica Acta*, 12(10), pp. 1421-1428.

10. Bazán, J. C., Arvia, A.J. (1964). *Electrochim Acta*, 9(5), pp. 667-684.

11. Levich, B. (1947). *Discuss. Faraday Soc*., 1, pp. 37-49.

12. Newman, J. (1973). *Electroanalytical Chemistry*, 6, pp. 279-297.

13. Whitaker, D., Nelson, J. B., Schwartz, D. T. (2005). *J. Micromech, Microeng*, 15, pp. 1498.

14. Nelson, J. B., Wisecarver, Z., Schwartz, D.T. (2007). *J. Micromech, Microen.*, 17, pp. 1192.

15. Schoenenberger, I., Roy,S. (2005). *Electrochim Acta*, 51(1) pp. 809-819.

16. Wu, Q.-B., Green, T. A., Roy, S. (2011). *Electrochem. Comm*, 13(11), pp. 1229-1232.

17. Nouraei, S., Roy, S. (2008). *J. Electrochem. Soc*., 155, pp. D97-D103.

18. Tsuda, T., Hussey, C.L. (2007). Electrochemical Applications of Room-Temperature Ionic Liquids. I*nterface*.

19. Endres, F., MacFarlane, D., Abbott, A. (2017). Electrodeposition from Ionic Liquids. (eds.), Wiley-VCH: Weinheim.

20. Valverde-Armas, P., Green, T., Roy, S. (2018). *J. Electrochem. Soc*., 165(9), pp. D313-320.

21. Pollet, B.G (2012). Power Ultrasound in Electrochemistry: From Versatile Laboratory Tool to Engineering Solution. Chichester: John Wiley & Sons.

22. Compton, R.G., Eklund, J.C., Page, S.D., Mason, T.J., Walton, D.J. (1996). *J. Appl. Electrochem*, 26, pp. 775-784.

23. Serra, A., Coleman, S.J., Gomez, E., Green, T.A., Valles, E., Vilana, J., Roy, S. (2016). *Electrochimica Acta*, 207, pp. 207-217.

24. Jensen, J.A.D., Pocwiardowski, P., Persson, P.O. Å., Hultmann, L., Møller, P. (2003). *Chemical Physics Letters*, 368, pp. 732-737.

25. Ohsaka, T., Goto, Y., Sakamoto, K., Isaka, M., Imabayashi, S., Hirano, K. (2010). *Trans. Institute of Metal Finishing*, 88(4), pp. 204-208.

26. Cravotto, G., Cintas, P. (2012). *Chemical Science*, 3, pp. 295-307.

27. Birkin, P.R., O'Connor, R., Rapple, C. and Martinez, S.S. (1998). *Journal of the Chemical Society, Faraday Transactions*, *94*(22), pp. 3365-3371.

28. Lorimer, J.P., Pollet, B., Phull, S.S., Mason, T.T., Walton, D.J., Geissler, U. (1996). *Electrochim Acta*, 41 (17), pp. 2737-2741.

29. Pollet, B.G., Hihn, J.Y., Doche, M.L., Lorimer, J.P., Mandroyan, A., Mason, T.J. (2007). *J. Electrochem. Soc.*, 154(10), pp. E131-E138.

30. Eklund, J.C, Marken, F., Waller, D.N., Compton, R.G. (1996). *Electrochim Acta*, 41(9), pp. 1541-1547.

31. Marken, F., Compton, R.G. (1996). *Ultrasonics Sonochemistry*, 3(2), pp. S131-S134.

32. Coleman, S.J., Roy, S. (2014). *Chemical Engineering Science*, 113, pp. 35-44.

33. Coleman, S.J. (2015). Thesis: Scale-Up of Enface Electrochemical Reactor Systems. Newcastle University.

34. Csoka, L., Katekhaye, S.N., Gogate, P.R. (2011). *Chemical Engineering Journal*, 178, pp. 384-390.

35. Coleman, S.J., Roy, S. (2018). *Ultrasonics–Sonochemistry*, 42, pp. 445-451.

36. Benjamin, T.B., Ellis, A.T. (1966). *Philosophical Transactions of the Royal Society of London. Series A, Mathematical and Physical Sciences*. 260, pp. 1110.

37. Kudo, N., Okada, K., Yamamoto, K. (2009). *Biophysical Journal*, 96(12), pp. 4866–4876.

38. Tsochatzidis, N.A., Guiraud, P., Wilhelm, A.M., Delmas. H. (2001) *Chemical Engineering Science,* 56, pp. 1831-1840.

39. Struyf, H., Mertens, P., Heyns, M., De Gendt, S., Glorieux, C., Brems, S. (2013) *Ultrasonics – Sonochemistry*, 20, pp. 77-88.